Biointerface Research in Applied Chemistry
Platinum Open Access Journal (ISSN: 2069-5837)

Article
Volume 12, Issue 6, 2022, 8105 - 8116
https://doi.org/10.33263/BRIAC126.81058116

Antibacterial Studies of Penicillin G Loaded Carboxylic Cellulose Acetate Nanoparticles

Boon-Kui Ho [1], Suk-Fun Chin [1,*], Samuel Lihan [2]

1 Faculty of Resource Science and Technology, Universiti Malaysia Sarawak 94300, Kota Samarahan, Sarawak, Malaysia;
2 Institute of Biodiversity and Environmental Conservation, Universiti Malaysia Sarawak 94300, Kota Samarahan, Sarawak Malaysia
* Correspondence: sfchin@unimas.my (S.F.C);

Scopus Author ID 16644797900
Received: 5.10.2021; Revised: 15.11.2021; Accepted: 19.11.2021; Published: 9.12.2021

Abstract: Cellulose acetate nanoparticles (CCA NPs) with mean particles sizes of 97 nm were synthesized via the nanoprecipitation process. The antibacterial properties of these CCA NPs were evaluated against Gram (+) and Gram (-) bacteria, respectively. The CCA NPs exhibited good antibacterial activity against Methicillin-resistant Staphylococcus aureus (MRSA) (+), Staphylococcus epidermis (+), Escherichia coli (-), Bacillus cereus (+), and Salmonella typhimurium (-) in range of MIC of 2.5×102 to 5.0×102 µg.mL-1 and MBC of 5.0×102 to 1.0×103 µg.mL-1. Penicillin G (PenG)-loaded CCA NPs demonstrated synergistic antibacterial activities against Gram (+) and Gram (-) bacteria. PenG-loaded CCA NPs also exhibited promising antimicrobial activity against the Methicillin-resistant staphylococcus aureus (MRSA) superbug, which is resistant to penicillin G. These promising antibacterial properties suggested that CCA NPs could potentially serve as an alternative potent antimicrobial agent for both Gram (+) and Gram (-) bacteria as well as the superbug MRSA.

Keywords: cellulose nanoparticles; penicillin-loaded cellulose nanoparticles; antibacterial activity; Methicillin-resistant *staphylococcus aureus* (MRSA); superbug.

1. Introduction

Even though there are many types of antibiotics available in the market for the treatment of bacterial infections, however, most of the bacteria tend to evolve into mutated antibacterial-resistant bacteria. For instance, *Staphylococcus aureus* evolved and mutated into MRSA superbugs. Furthermore, misuse and overdosage of antibiotics may lead to bacteria resistance towards antibiotics, reduce the effectiveness, and ultimately lead to the emergence of new infections. Therefore, the search for a potential cure for MRSA infection is still a big challenge, and the development of new antibacterial agents has become an urgent need to treat infectious diseases.

Recently, polysaccharide-based nanoparticles have been studied extensively for biological applications due to their non-toxic, low cost, good biocompatibility, renewable and biodegradable [1,2]. Also, antimicrobial studies of polysaccharide-based nanoparticles were widely reported. For instance, Ismail and Gopinath [3] reported that starch nanoparticles loaded with penicillin and streptomycin were fabricated *via* the microemulsion method and evaluated for their antimicrobial activity against *Streptococcus pyogenes* and *Escherichia coli*. The result displayed an inhibition zone of 17 mm at the concentration of 1 mg/mL. Another similar study was also reported by Gopinath *et al*. [4] on the preparation of ampicillin-loaded cellulose

nanoparticles and applied for antimicrobial activity against *Escherichia coli*. The result showed a good inhibition zone of 20 mm. In addition, cellulose can also absorb toxins produced by bacteria and enhance the drugs' effectiveness [5]. However, unmodified cellulose has its limitations due to its weakness of hydration, structural organization, and lack of antimicrobial activity [6,7]. Therefore, modification of cellulose is of vital importance to impart functionality and antimicrobial properties for various biomedical applications [8].

Based on previous studies, several antibacterials studies of antibiotics-loaded cellulose derivatives nanoparticles have been reported. For instance, Panin *et al*. [9] reported on the preparation of clarithromycin-loaded ethyl cellulose nanoparticles, which exhibited excellent antibacterial activity against *H.pyrori* by binding to the HEp-2 cell. Besides that, another study related to antibiotic-loaded polymeric nanoparticles was also reported. Farrukh *et al*. [10] prepared ciprofloxacin (CIP)-loaded diethylaminoethyl cellulose nanoparticles and evaluated them for their antimicrobial activity against *E.coli* and pathogenic *staphylococci* with an inhibition zone of 27 mm and 14 mm, respectively.

In this study, the antimicrobial activity of the PenG-loaded CCA NPs against gram-positive and gram-negative bacteria was studied and evaluated. Therefore, this investigation also aimed to evaluate new possible PenG-loaded CCA NPs to act as promising candidate nanoparticles-based antibacterial against superbugs Methicillin-resistant *staphylococcus aureus* (MRSA).

2. Materials and Methods

The materials used in this work: CCA NPs containing 16.2 % carboxyl groups (w/w) and DS of acetyl at 1.95 was prepared according to the reported procedure [11], phosphate buffer solution (PBS), ethanol, penicillin G were supplied from Fisher Scientific, 3-(4,5-dimethylthiazol-2-yl)-2,5-diphenyltetrazolium bromide (MTT), Mueller-Hinton broth (MHB) was purchased from OXOID brand, Mueller-Hinton agar (MHA) was purchased from Merck company, Ultrapure water (~18.2 MΩ.cm, 25 °C) was prepared using the Water Purifying System (ELGA Model Ultra Genetic). All chemicals were used without further purification.

Preparation of CCA NPs: the dried powdered CCA was dispersed in 10 mL of ultrapure water and added dropwise into 30 mL ethanol *via* the nanoprecipitation process. The resulting mixtures were centrifuged at 1250 rpm, and the supernatant was removed to obtain CCA NPs. The CCA NPs, were rinsed three times with absolute ethanol and dried in a conventional oven at 60 ˚C overnight. A measured expanse of nanoparticles was dispersed in absolute ethanol, and a drop of the dispersed sample was drop coated onto formvar-coated copper grids. The morphology of samples was characterized and observed under a transmission electron microscope (TEM) (JEOL Model1230).

Penicillin G loading: CCA NPs (100 mg) were immersed in phosphate buffer saline (PBS, pH 7.4), which contained PenG (1 mg/mL), and incubated at 37 ˚C for 72 h until equilibrium absorption was achieved.

$$\text{Loading capacity (mg.mg}^{-1}) = \frac{\text{PenG}_{ini} - \text{PenG}_{free}}{\text{weight of CCA NPs}} \quad (1)$$

where, PenG_{ini} (mg) is the initial amount of penicillin G used, and PenG_{free} (mg) is the amount of penicillin G remaining in the supernatant.

After a specific time interval, the absorbance of the solution containing the residual drug was measured spectrophotometrically using a UV/Vis spectrophotometer at 212 nm. The molar concentration of penicillin G was calculated from the absorbance values, according to a standard calibration curve in PBS solution. The loading capacity of PenG for CCA NPs was calculated using the following equation (1) [12].

Antibacterial activities: the antibacterial activities of samples were evaluated against Gram (-) pathogenic bacteria (*Escherichia coli* (-), and *Salmonella typhimurium* (-)) and Gram (+) pathogenic bacteria (*Methicillin-resistant staphylococcus aureus* (MRSA) (+), *Staphylococcus epidermis* (+), *Bacillus cereus* (+)). Each bacteria strain was cultured in Mueller Hinton broth (MHB) medium and incubated at 37 °C for 24 h to be used as inoculums before being applied to the antibacterial assay of good diffusion, minimum inhibition concentration (MIC), and minimum bactericidal concentration (MBC) analyses. All the methods applied to evaluate the antibacterial activity were according to the Clinical and Laboratory Standards Institute (CLSI) protocol [13].

PenG-loaded CCA NPs were tested for antibacterial activity *via* well diffusion assay against the Gram (+) and Gram (-) pathogenic bacteria. The pure cultures of bacteria (1×10^6 $CFU.mL^{-1}$) were sub-cultured on MHA and were swabbed uniformly onto the individual plates using sterile cotton swabs. Subsequently, wells were punched into the agar medium by a sterile straw and filled with 75 µL of samples (1.0×10^3 $\mu g.mL^{-1}$). PenG is used as a positive control. Bacterial-cultured (Gram-negative) plates and bacterial-cultured (Gram-positive) plates were incubated in the upright position at 37°C for 24 h and 18 h, respectively. The diameter of the inhibition zone was measured with a ruler.

Minimum inhibitory concentration (MIC) assay was performed *via* the microdilution method with slight modifications. Each 100 µL of samples of known concentration prepared was added into 96 well round-bottomed microtiter plates containing 100 µL of Muller Hinton broth (MHB) medium. Dilutions were carried out by a two-fold serial dilution approach. Then, 100 µL of tested microorganisms bacteria (1×10^6 $CFU.mL^{-1}$) were inoculated to all wells, and the microtitre plates were incubated at 37°C for 24 h. After the incubation of 24 h, 3-(4,5-dimethylthiazol-2-yl)-2,5-diphenyltetrazolium bromide (MTT) was subsequently added to 96 wells and incubated again at 37 °C for an hour. The optical densities of cultures are read at 540 nm using a microplate reader (Biorad Model 680). From the absorbance of optical densities (OD), the minimum inhibitory concentration was determined as the lowest concentration of samples that inhibits the growth of bacteria [14]. The reduction of bacteria was calculated in percentage according to equation (2) shown below:

$$\text{Percentage of bacteria reduction (\%)} = 1 - (OD_{test}/OD_{control}) \times 100\ \% \quad (2)$$

where, OD_{test} is the optical density of microorganisms treated with sample and $OD_{control}$ is the optical density of microorganisms untreated with sample.

Minimum bactericidal concentration (MBC) was determined from minimum inhibitory concentration (MIC) that did not reveal any visible growth of bacteria colonies from the microtitre wells after 24 h of incubation [15]. The inhibition of bacterial growth was assessed by comparing the optical density of samples to normal growth of culture (untreated with prepared samples) in the control wells. Briefly, exactly 5 µL of the mixture from serial dilution of microtitre wells with no sign of turbidity was pipetted onto the MHA agar plates and incubated at 37°C for 24 h. The bacteria growth on the plate was then observed.

All experiments and analyses were carried out in triplicate. Statistical analysis was accomplished using Microsoft Excel, and results are expressed as mean ± standard error (SE).

3. Results and Discussion

3.1. Preparation of PenG-loaded CCA NPs route for antibacterial assay.

As shown in Figure 1, prepared CCA NPs were loaded with antibiotics (PenG) *via* immersion process under incubation at 37 °C for 72 h. The highest PenG loading capacity was evaluated for antibacterial activity against Gram (+) and Gram (-) bacteria, respectively, and provides a release of the PenG to inhibit and deactivate bacteria strains. Also, CCA NPs contribute towards enhancing antibacterial efficiency.

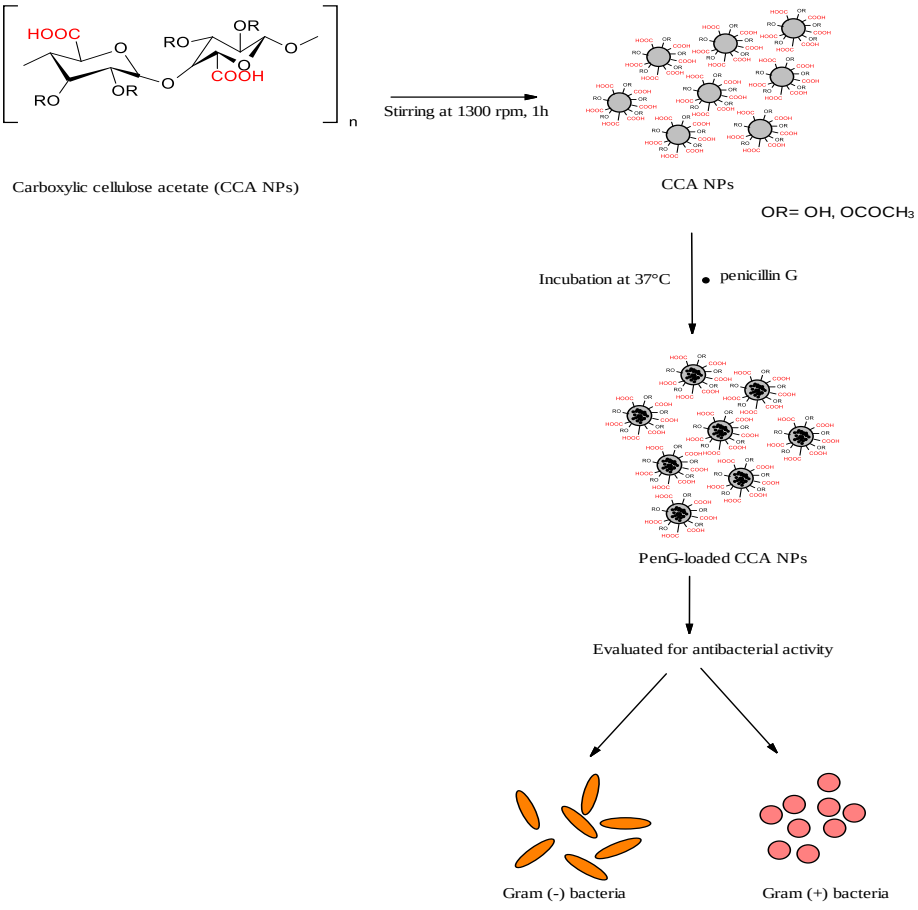

Figure 1. Schematic representation of prepared PenG-loaded CCA NPs route applied for antibacterial activity against Gram (-) bacteria and Gram (+) bacteria.

3.2. Surface morphology of CCA NPs and PenG-loaded CCA NPs

As shown in Figure 2 (a), the TEM image showed that the nanoparticles were spherical particles with a mean particles size of 91 nm, while loading of penicillin G onto CCANPs, PenG-loaded CCA NPs were observed to have a spherical shape with a mean particles size of 200 nm based on the TEM micrograph shown in Figure 2 (b). It is because most PenG was absorbed into CCA NPs could lead to the particles size enlarged. This showed that the loading of the antibiotic onto nanoparticles could lead to the increased particles size of the nanoparticles.

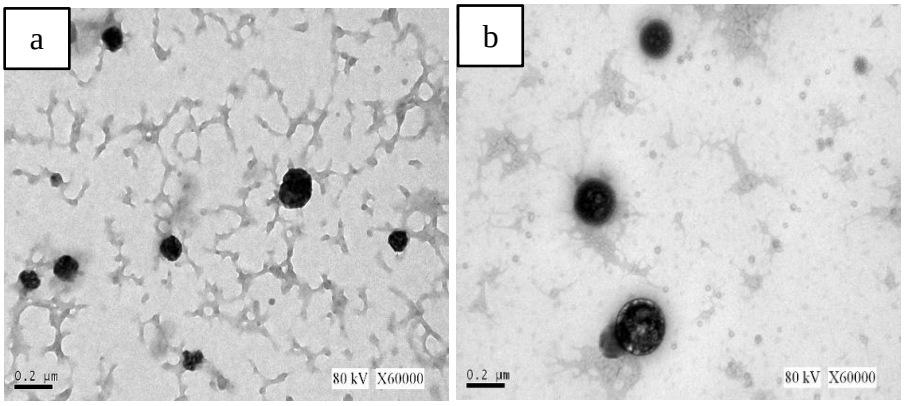

Figure 2. TEM micrographs of **(a)** CCA NPs**, (b)** PenG-loaded CCA NPs.

3.3. Loading capacity.

As shown in Figure 3, the loading of PenG was observed to increase very rapidly initially between the loading duration of 0 and 8 h. This could be attributed to the initial migration of the drug solution into the CCA NPs until the CCA NPs were wet enough, after which the PenG could be loaded quickly until saturation. However, the loading slowed down gradually between 8 h and 16 h, eventually maintaining the loading capacity after incubation for 32 h or longer. It is because CCA NPs almost being fully occupied by drug molecules. Hence, the maximum loading capacity of PenG was observed at 0.66 $mg.mg^{-1}$ after 72 h. Subsequently, PenG-loaded CCA NPs were evaluated for antibacterial activity against Gram (+) and Gram (-) bacteria.

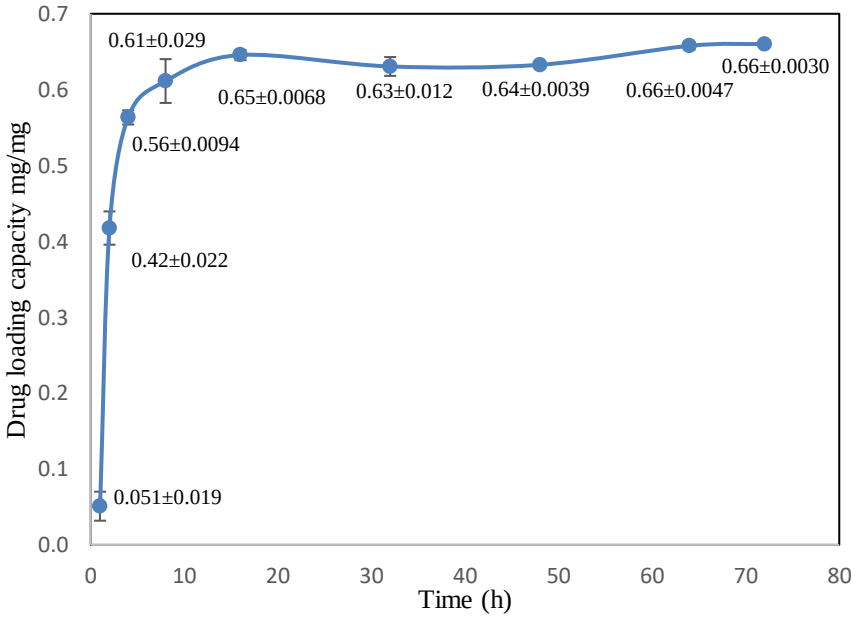

Figure 3. The loading capacity of PenG onto CCA NPs as a function of loading duration.

3.4. Antibacterial activities of CCA NPs, and PenG-loaded CCA NPs.

Pathogenic bacterial infection is one of the major infectious diseases that lead to globally severe illness and plague to healthcare [16]. Especially, methicillin-resistant *Staphylococcus aureus* (MRSA) was listed as important pathogens causing severe community in the World Health Organization's priority pathogens list for investigation and development of new antibacterial agents [17, 18]. MRSA is a bacterium that causes infections in different body parts and is hard to treat with antibiotics [19, 20]. Based on a previous study, MRSA

produced an enzyme that could hydrolyze the β-lactam ring in antibiotic molecules, thus deactivating the function of antibiotics [21]. MRSA is also called a "superbug" due to its resistance to the most commonly used antibiotics [22]. Due to MRSA's medical importance, MRSA is still investigated in many surveillance initiatives [23-26]. Therefore, the enhancement or development of new antibacterial agents has become urgently needed for the treatment of bacterial infectious diseases. Interestingly, CCA NPs were found to be a good antibacterial agent against MRSA and also other bacteria such as Gram (+) bacteria (*Staphylococcus epidermis*, and *Bacillus cereus*) and Gram (-) bacteria (*Salmonella typhimurium*, and *Escherichia coli*), respectively. According to the results of antibacterial activities presented in Table 1 and Figure 4 (b and c), PenG-loaded CCA NPs exhibited a more superior antibacterial effect against *Salmonella typhimurium*, and *Escherichia coli* with an inhibition zone of 12 and 13 mm, respectively compared to CCA NPs.

Further determination of MIC and MBC values which recorded in Table 2, PenG-loaded CCA NPs revealed MIC values of 2.5×10^2 µg/mL against both *Salmonella typhimurium* , and *Escherichia coli*, while MBC of PenG-loaded CCA NPs against *Salmonella typhimurium*, and *Escherichia coli* with the values of 1.0×10^3 and 5.0×10^2 µg/mL, respectively which shown in Figure 5 (a and e). Based on the previous studies, Gram (-) bacteria have peptidoglycan between membranes, which results in an antibacterial agent that is difficult to pass through compared to Gram (+) bacteria, consisting of a peptidoglycan layer on the outside of the cell wall [27, 28]. However, it is composed of a protein channel on the outer membrane of the cell wall [29, 30]. Several protein channels could be affected by negatively charged ions from a carboxylic acid (COOH), which could increase the membrane permeability on bacteria's cell wall. The carboxylic of CCA NPs could produce proton (H^+). This H^+ could diffuse into the bacteria's cytoplasm to lower internal pH, disrupting bacteria cellular adenosine triphosphate (ATP) which, produced energy and resulted in the depletion of energy in bacteria [31, 32]. Therefore, the bacteria cells are inhibited and damaged. Also, this allows the diffusion of H^+ ions from COOH into the plasma membrane, which results in the leakage of protein from the membrane bacteria [33, 34]. At this point, PenG molecules released from PenG-loaded CCA NPs could easily pass through the outer cell wall and inhibit the peptidoglycan layer of the bacteria from stopping the growth of bacteria cells [33, 35, 36]. Furthermore, acetate from CCA NPs could penetrate through the cell membrane into the cytoplasm. Roe *et al*. [37] concluded that acetate anions treated bacteria cells may inhibit the activity of a protein and led to the accumulation of homocysteine which is the last intermediate on the methionine biosynthetic pathway. Thus homocysteine was found to inhibit the growth of *Escherichia coli*. Therefore, this has shown that PenG loaded onto CCA NPs could enhance its antibacterial activity.

On the other hand, Gram (+) bacteria consisted of a peptidoglycan layer outside of the cell wall but lacked an outer membrane compared to Gram (-) bacteria [29]. Because of this, PenG molecules could penetrate through the outer cell wall easily to reach the peptidoglycan layer of the bacteria [38]. PenG molecules consist of β-lactam, which could interact with peptidoglycan targeted sites and inhibit peptidoglycan biosynthesis. As a result, the formation of a new cell wall of microorganisms could be avoided [39, 40]. From Table 1 and Figure 4 (a), the PenG and CCA NPs against *S. epidermis* have shown the value of inhibition zone with a diameter of 15 and 13 mm, respectively. This had shown that PenG could produce a good antibacterial effect against *S. epidermis*. Therefore, the *S. epidermis* strain was able to be inhibited by PenG well compared to CCA NPs. In addition, PenG-loaded CCA NPs could produce a better antibacterial effect against *Staphylococcus epidermis* with a diameter

inhibition zone of 14 mm compared to CCA NPs. This has proven that CCA NPs loaded with penicillin G have the potential to enhance antibacterial activity. Table 2 also showed that PenG-loaded CCA NPs had produced a lower value of MIC with 1.25×10^2 µg/mL against *Staphylococcus epidermis* compared to CCA NPs with MIC of 2.5×10^2 µg/mL. Therefore, the PenG-loaded CCA NPs against *Staphylococcus epidermis* with a reduced growth rate of 97.53%. Similarly, PenG-loaded CCA NPs also showed good antibacterial activity against *Bacillus cereus* with an inhibition zone of 12 mm compared to both PenG and CCA NPs with an inhibition zone of 9 mm. Further evaluated by MIC and MBC analysis which is shown in Table 2 and Figure 5 (c), PenG-loaded CCA NPs had shown the lower value of MIC and MBC value of 1.25×10^2 and 5.0×10^2 µg/mL, respectively, against *Bacillus cereus*. This has proved that loading of PenG onto CCA NPs could exhibit better antibacterial effects which are necessary to inhibit those bacteria cells.

However, antibiotics such as PenG are less effective against MRSA due to MRSA has mutated *Staphylococcus aureus*, which is highly resistant to antibiotics containing methicillin molecule [22]. PenG against MRSA with an only exhibited inhibition zone of 8 mm which is revealed in Table 1 and Figure 4 (d). This smaller inhibition zone of PenG against MRSA is due to MRSA being able to produce a penicillin-binding protein (PBP2a) which is resistant to β-lactam ring in PenG, and stop the inhibitory effect of the PenG [41, 42]. Therefore, MRSA can be resistant to all antibiotics that contain β-lactam ring structure and deactivate the functions of the antibiotic [43, 44, 45, 46]. In contrast, CCA NPs against MRSA has a better inhibition zone of 17 mm than PenG alone. Since CCA NPs had exhibited good antibacterial activity against MRSA.

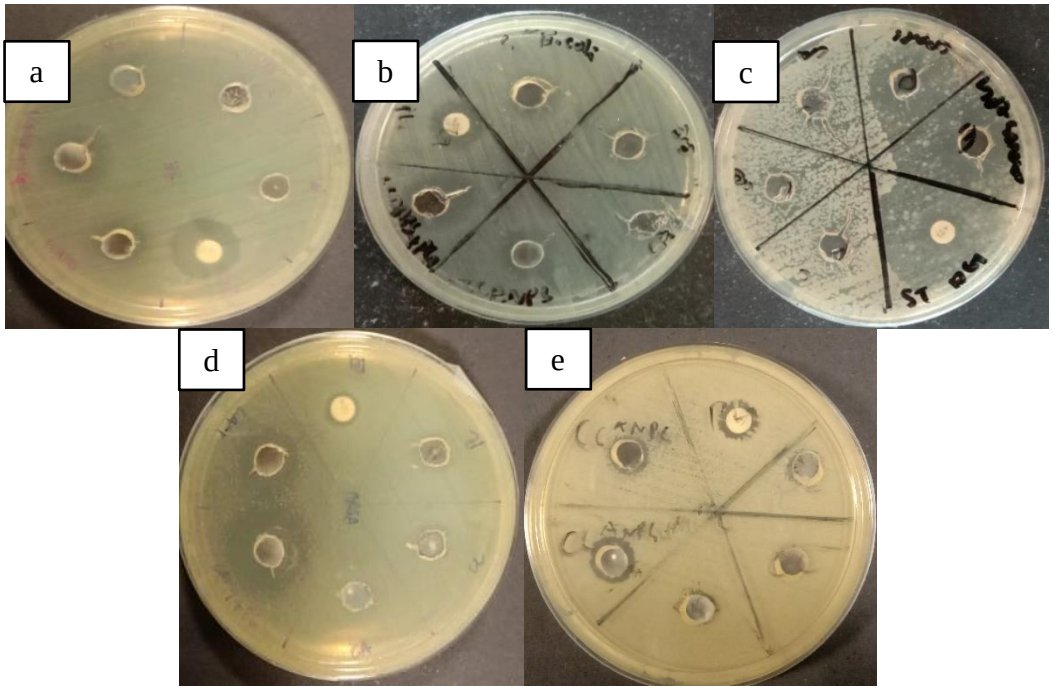

Figure 4. Screening of antibacterial activity using well diffusion method against **(a)** *Staphylococcus epidermis*, **(b)** *Escherichia coli*, **(c)** *Salmonella typhimurium* **(d)** Methicillin-resistant *staphylococcus aureus* (MRSA) and **(e)** *Bacillus cereus.*

Notably, PenG loaded onto CCA NPs had exhibited an excellent antibacterial effect against MRSA with larger values of inhibition zone diameter, which was 20 mm compared to both PenG and CCA NPs and further determined by MIC and MBC of PenG-loaded CCA NPs against MRSA which recorded in Table 2 and Figure 5 (d).

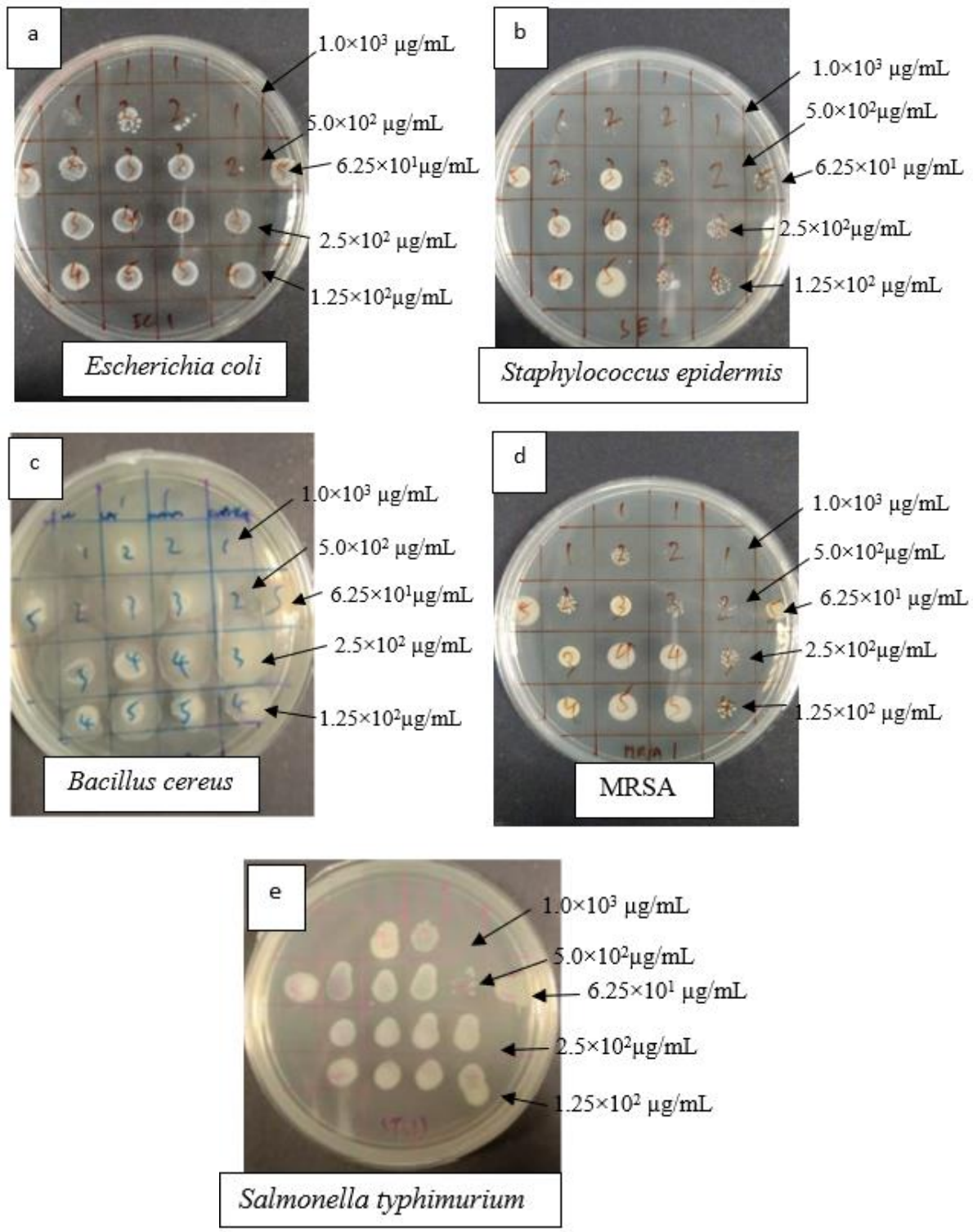

Figure 5. MBC of **(a)** *Escherichia coli*, **(b)** *Staphylococcus epidermis*, **(c)** *Bacillus cereus*, **(d)** Methicillin-resistant *staphylococcus aureus* (MRSA), and **(e)** *Salmonella typhimurium.*

Table 1. Diffusion assay of pure cellulose, carboxylic cellulose, cellulose acetate, CCA NPs, PenG, and PenG-loaded CCA NPs (n = 3), P<0.05.

Bacteria strains	Inhibition zone diameter (mm)					
	Pure cellulose	Carboxylic cellulose	Cellulose acetate	PenG	CCA NPs	PenG-loaded CCA NPs
Bacillus cereus (+)	0	0	0	9±0.0	9±0.0	12±0.82
Methicillin resistant *staphylococcus aureus* (MRSA) (+)	0	0	0	8±0.0	17±0.47	20±0.82
Escherichia coli (-)	0	0	0	12±0.0	11±0.82	13±1.6
Salmonella thypimurium (-)	0	0	0	9±0.0	11±0.82	12±0.0
Staphylococcus epidermis (+)	0	0	0	15±0.0	13±0.0	14±1.6

Table 2. MIC, MBC and reduction growth (%) of CCA NPs, PenG and PenG-loaded CCA NPs (n = 3), P<0.05.

	PenG			CCA NPs			PenG-loaded CCA NPs		
Bacteria strains	**MIC (μg.mL^{-1})**	**MBC (μg.mL^{-1})**	**Reduction Growth (%)**	**MIC (μg.mL^{-1})**	**MBC (μg.mL^{-1})**	**Reduction growth (%)**	**MIC (μg.mL^{-1})**	**MBC (μg.mL^{-1})**	**Reduction Growth (%)**
Salmonella thymius (-)	2.5×10^{2}	5.0×10^{2}	94.12±0.48	5.0×10^{2}	1.0×10^{3}	90.19±0.24	2.5×10^{2}	1.0×10^{3}	94.89±1.42
Methicillin resistant *staphylococcus aureus* (MRSA) (+)	2.5×10^{2}	5.0×10^{2}	94.83±1.09	2.5×10^{2}	5.0×10^{2}	94.78±0.6	1.25×10^{2}	5.0×10^{2}	98.63±0.62
Escherichia coli (-)	1.25×10^{2}	2.5×10^{2}	93.44±0.68	5.0×10^{2}	1.0×10^{3}	90.61±0.26	2.5×10^{2}	5.0×10^{2}	93.71±0.61
Bacillus cereus (+)	2.5×10^{2}	5.0×10^{2}	92.18±0.33	2.5×10^{2}	5.0×10^{2}	89.62±0.68	1.25×10^{2}	5.0×10^{2}	92.50±0.60
Staphylococcus epidermis (+)	6.25×10^{1}	1.25×10^{2}	97.27±0.59	2.5×10^{2}	5.0×10^{2}	90.42±0.63	1.25×10^{2}	5.0×10^{2}	97.53±0.64

It was shown that PenG-loaded CCA NPs could enhance antibacterial effect against MRSA with lower values of MIC and MBC which were 1.25×10^{2} and 5.0×10^{2} μg/mL, respectively, compared to both CCA NPs and PenG alone. In addition, the reduction growth of MRSA (98.63%) with PenG-loaded CCA NPs had shown a great enhancement in antibacterial effect compared to PenG alone (94.83%).

Figure 6 (a) and (b) compared the morphology of bacteria before and after being treated with PenG-loaded CCA NPs. The shape of MRSA bacteria cells was disrupted and damaged after being treated with PenG-loaded CCA NPs compared to untreated MRSA. The antibacterial mechanism of this phenomenon could be due to the proton (H^{+}) produced from COOH, which could diffuse into the bacteria's cytoplasm to lower internal pH, disrupted bacteria cellular adenosine triphosphate (ATP) which, produced energy and resulted in depletion of energy in bacteria [31]. Furthermore, acetate anion produced from CCA NPs also diffused into the cell membrane and led to the inhibition of enzyme activity by the accumulating acetate anions. Wei *et al.* [47] reported that acetate ion could inhibit *Staphylococcus aureus* by inhibiting protein transcription factor called *nuclear factor kappa B* (NF-kB), and deactivating it. PenG released from CCA NPs could pass through the outer cell wall and inhibit peptidoglycan synthesis, which could terminate the growth of bacteria cells [39].

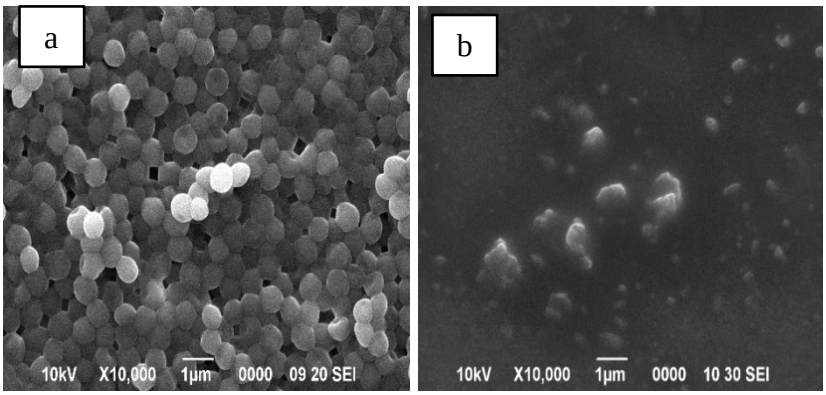

Figure 6. SEM of micrographs of **(a)** Methicillin-resistant *staphylococcus aureus* (MRSA) before treated on MHA agar plate **(b)** Methicillin-resistant *staphylococcus aureus* (MRSA) after treated with PenG-loaded CCA NPs.

4. Conclusions

In this study, the antibacterial property of CCA NPs has been evaluated. CCA NPs showed great potential as a promising antibacterial agent, and PenG-loaded CCA NPs displayed synergistic antibacterial effect against Gram (-) and Gram (+) bacteria strains and the Methicillin-resistant *Staphylococcus aureus* (MRSA) superbug. The mechanism underlying the antibacterial activity was due to the dissociation of H^+ from CCA NPs, which decreased the pH of bacteria cells and disrupted the cells membrane. Furthermore, acetate ions could inhibit the growth of bacteria cells by deactivating the protein of bacteria. Given the various unique properties of cellulose-based nanoparticles such as low toxicity, biodegradability, abundance, high surface to volume ratio, and excellent antibacterial properties, CCA NPs and PenG loaded CCA NPs were envisaged to be the potential nanoparticles-based antibacterial agents for the effective treatment of bacterial infections.

Fundings

This work was supported by the Fundamental Research Grant Scheme (FRGS), Ministry of Higher Education, Malaysia (Grant No: FRGS/1/2016/STG01/UNIMAS/01/1).

Acknowledgments

Boon-Kui Ho would like to express his gratitude to University Malaysia Sarawak (UNIMAS) Zamalah for his Ph.D. scholarship.

Conflicts of Interest

The authors declare no conflict of interest.

References

1. Chin, S. F.; Jimmy, F.B.; Pang, S.C. Size controlled fabrication of cellulose nanoparticles for drug delivery applications. *Journal of Drug Delivery Science and Technology*. **2017**, *43*, 262-266, https://doi.org/10.1016/j.jddst.2017.10.021.
2. Pang, S.C.; Chin, S.F.; Yih, V. Conversion of cellulosic waste materials into nanostructured ceramics and nanocomposites. *Advanced Materials Letters*. **2011**, *2*, 118-124, https://doi.org/10.5185/amlett.2011.1203.
3. Ismail, N.S.; Gopinath, S.C.B. Enhanced antibacterial effect by antibiotic loaded starch nanoparticle. *Journal of the Association of Arab Universities for Basic and Applied Sciences*. **2016**, *1*, 1-5, https://doi.org/10.1016/j.jaubas.2016.10.005.
4. Gopinath, S.C.B.; Goh, C.S.; Citartan, M.; Lakshmipriya, T.; Arshad, M.K.M.; Faudzi, F.N.M.; Rahim, R.A.; Hashim, U.; Chinni, S.V.; Tang, T.H. Micro-encapsulation of antibiotic in cellulose nanoparticle inhibits bacteria. *Micro and Nanosystems*. **2016**, *8*, 41-46, https://doi.org/10.2174/1876402908666160720104019.
5. Yoo, B. K.; Chen, J. Role of cellulose in protecting Shiga toxin producing *Escherichia coli* against oxidative and acidic stress. *Food control*. **2012**, *23*, 289-292, https://doi.org/10.1016/j.foodcont.2011.07.016.
6. Chin, S.F.; Makha, M.; & Raston, C.L.; Saunders, M. Magnetite ferrofluids stabilized by sulfonato-calixarenes. *Chemical Communications*, **2007**, *19*, 1948-1950, https://doi.org/10.1039/B618596G.
7. Voon, L.K.; Pang, S.C.; Chin, S. F. Regeneration of cello-oligomers via selective depolymerization of cellulose fibers derived from printed paper wastes. *Carbohydrate Polymers.* **2016**, *142*, *31–37*, https://doi.org/10.1016/j.carbpol.2016.01.027.
8. Chin, S.F.; Romainor, A.N.B.; Pang, S.C.; Lihan, S. Antimicrobial starch-citrate hydrogel for potential applications as drug delivery carriers. *Journal of Drug Delivery Science and Technology*. **2019**, *54*, 101239–101247, https://doi.org/10.1016/j.jddst.2019.101239.
9. Panin, P.; Banlunara, W.; Chaichanawongsaroj, N. Ethyl cellulose nanoparticles : Clarithomycin encapsulation and eradication of H. pylori. *Carbohydrate Polymers.* **2014**, *109*, 22–27, https://doi.org/10.1016/j.carbpol.2014.03.025.

10. Farrukh, M. A.; Gul, M. R.; Rahman, M.K. Ciprofloxacin loaded diethylaminoethyl cellulose nanoparticles. **2017**. US20160106685A1 (Patent), https://patents.google.com/patent/US20160106685A1/en.
11. Ho, B.K.; Chin, S.F.; Pang, S.C. pH-responsive carboxylic cellulose acetate nanoparticles for controlled release of penicillin G. *Journal of Science Advanced Materials and Devices*. **2020**, *5*, 224–232, https://doi.org/10.1016/j.jsamd.2020.04.002.
12. Chang, Y.; Meng, X.; Zhao, Y.; Li, K.; Zhao, B.; Zhu, M.; Li, Y.; Chen, X.; Wang, J. Novel water-soluble and pH-responsive anticancer drug nanocarriers: doxorubicin–PAMAM dendrimer conjugates attached to superparamagnetic iron oxide nanoparticles (IONPs). *J Colloid Interface Sci*. **2011**, *363*, 403–409, https://doi.org/10.1016/j.jcis.2011.06.086.
13. CLSI, Performance Standards for Antimicrobial Disk Susceptibility Tests, Approved Standard, 7th ed., CLSI document M02-A11. Clinical and Laboratory Standards Institute, 950 West Valley Road, Suite 2500, Wayne, Pennsylvania 19087, USA, **2012**, https://www.researchgate.net/file.PostFileLoader.html?id=58139aa4615e27240754da03&assetKey=AS%3A422233756704774%401477679780485.
14. Qi, L.; Xu, Z.; Jiang, X., Hu, C.; Zou, X. Preparation and antibacterial activity of chitosan nanoparticles. *Carbohydrate Research*. **2004**, *339*, 2693-2700, https://doi.org/10.1016/j.carres.2004.09.007.
15. Dulger, G.; Aki, C. Antimicrobial activity of the leaves of endemic stachys pseudopinardii in turkey. *Tropical Journal of Pharmaceutical Research*. **2009**, *8*, 371-375, https://doi.org/10.4314/tjpr.v8i4.45231.
16. Spellberg, B.; Guidos, R.; Gilbert, D.; Bradley, J.; Boucher, H.W.; Scheld, W.M.; Bartlett, J. G.; Edwards, J.J. The epidemic of antibiotic-resistant infections: a call to action for the medical community from the Infectious Diseases Society of America. *Clin Infect Dis*. **2008**, *46*, 155–164, https://doi.org/10.1086/524891.
17. Ismail, M.A.H.; Kamarudin, N.; Abdul Samat, M.N.; Raja Abdul Rahman, R.M.F.; Saimun, S.; Tan, T.L.; Neoh, H.M. Methicillin-Resistant *Staphylococcus aureus* (MRSA) clonal replacement in a malaysian teaching hospital: findings from an eight-year interval molecular surveillance. *Antibiotics*. **2021**, *10*, 320-329, https://doi.org/10.3390/antibiotics10030320.
18. Cohen, R.; Paikin, S.; Finn, T.; Babushkin, F.; Anuka, E.; Baum, M.; Rokney, A. Molecular epidemiology of Methicillin-Resistant Staphylococcus aureus clinical isolates during 7.5 years in one regional hospital in israel. *Journal of Environmental and Public Health*. **2021**, *1*, 1-9, https://doi.org/10.1155/2021/6643108.
19. Chin, S.F.; Lim, L.S. ; Pang, S.C. ; Sum, M.S.H.; Perera, D. Carbon nanoparticle modified screen printed carbon electrode as a disposable electrochemical immunosensor strip for the detection of Japanese encephalitis virus. *Microchimica Acta*. **2017**, *184*, 491-497, https://doi.org/10.1007/s00604-016-2029-7.
20. Yao, Z.; Peng, Y.; Chen, X.; Bi, J.; Li, Y.; Ye, X.; Shi, J. Healthcare associated infections of methicillin-resistant Staphylococcus aureus: a case-control-control study. *Plos one*. **2015**, *10*, 1-9, https://doi.org/10.1371/journal.pone.0140604.
21. Guo, Y.; Song, G.; Sun, M.; Wang, J.; Wang, Y. Prevalence and therapies of antibiotic-resistance in *staphylococcus aureus*. *Frontiers in Cellular and Infection Microbiology*. **2020**, *1*, 1-11, https://doi.org/10.3389/fcimb.2020.00107.
22. Rajendran, R. Superbug infection. *Drug metabolism and Toxicology*. **2018**, *9*, 1-3, https://doi.org/10.4172/2157-7609.1000238.
23. Tsujiwaki, A.; Hisata, K.; Tohyama, Y.; Matsunaga, N.; Uehara, Y.; Sasaki, T.; Hiramatsu, K.; Shimizu, T. Epidemiology of methicillin resistant Staphylococcus aureus in a Japanese NICU. *Pediatrics International*. **2020**, *62*, 911-919, https://doi.org/10.1111/ped.14241.
24. Takaya, S.; Hayakawa, K.; Matsunaga, N.; Moriyama, Y.; Katanami, Y.; Tajima, T.; Tanaka, C.; Kimura, Y.; Saito, S.; Kusama, Y.; et al. Surveillance systems for healthcare-associated infection in high and upper-middle income countries: A scoping review. Off. *Journal of Japanese Society of Chemotherapy*. **2020**, *26*, 429-437, https://doi.org/10.1016/j.jiac.2020.01.001.
25. Pfaller, M.A.; Carvalhaes, C.G.; Smith, C.J.; Diekema, D.J.; Castanheira, M. Bacterial and fungal pathogens isolated from patients with bloodstream infection: Frequency of occurrence and antimicrobial susceptibility patterns from the SENTRY Antimicrobial Surveillance Program (2012–2017). *Diagnostic Microbiology and Infectious Disease* . **2020**, *97*, 115016-115023, https://doi.org/10.1016/j.diagmicrobio.2020.115016.
26. Coombs, G.W.; Daley, D.A.; Mowlaboccus, S.; Lee, Y.T.; Pang, S. Australian group on antimicrobial resistance (AGAR) australian *Staphylococcus aureus* sepsis outcome programme (ASSOP) annual report 2018. *Communicable Disease Intelligence*. **2020**, *44*, 1-17, http://dx.doi.org/10.33321/cdi.2020.44.18.
27. Sarwar, A.; Katas, H.; Samsudin, S.N.; Zin, N.M. Regioselective sequential modification of chitosan via azide-alkyne click reaction: synthesis, characterization, and antimicrobial activity of chitosan derivatives and nanoparticles. *PLoS One*. **2015**, *10*, 1-22, https://doi.org/10.1371/journal.pone.0123084.
28. Breijyeh, Z.; Jubeh, B.; Karaman, R. Resistance of gram-negative bacteria to current antibacterial agents and approaches to resolve it. *Molecules*. **2020**, *25*, 1340–1362, https://doi.org/10.3390/molecules25061340.
29. Brown, L.; Wolf, J.M.; Prados-Rosales, R.; Casadevall, A. Through the wall: extracellular vesicles in Gram positive bacteria, mycobacteria and fungi. *Nature reviews Microbiology*. **2015**, *13*, 620-630, https://doi.org/10.1038/nrmicro3480.

30. Alegun, O.; Pandeya, A.; Cui, J.; Ojo, I.; Wei, Y. Donnan potential across the outer membrane of gram-negative bacteria and its effect on the permeability of antibiotics. *Antibiotics*. **2021**, *10*, 701-716, https://doi.org/10.3390/antibiotics10060701.
31. Pinhal, S.; Ropers, D.; Geiselmann, J.; Jong, H.D. Acetate Metabolism and the Inhibition of Bacterial Growth by Acetate. *J Bacterio*. **2019**, *201*, 1-19, https://doi.org/10.1128/JB.00147-19.
32. Tran, T.T.T.; Kannoorpatti, K.; Padovan, A.; Thennadil, S. Sulphate-reducing bacteria's response to extreme pH environments and the effect of their activities on microbial corrosion. *Applied Science*. **2021**, *11*, 2201-2219, https://doi.org/10.3390/app11052201.
33. Chin, S.F.; Romainor, A.N. B.; Pang, S.C; Lihan, S. Antimicrobial starch-citrate hydrogel for potential applications as drug delivery carriers. *Journal of Drug Delivery Science and Technology*. **2019**, *54*, 1-9, https://doi.org/10.1016/j.jddst.2019.101239.
34. Liu, J.Y.; Du, C.l.; Beaman, H.T.; Monroe, M.B.B. Characterization of phenolic acid antimicrobial and antioxidant structure-property relationships. *Pharmaceutics*. **2020**, *12*, 419–.435, https://doi.org/10.3990/pharmaceutics12050419.
35. Ngu-Schwemlein, M.; Chin, S.F.; Hileman, R.; Drozdowski, C.; Upchurch, C.; Hargrove, A. Carbon nanodots as molecular scaffolds for development of antimicrobial agents. *Bioorganic Med. Chem. Lett*. **2016**, *26*, 1745–1749, https://doi.org/10.1016/j.bmcl.2016.02.047.
36. Wang, L.L.; Hu, C.; Shao, L,Q. The antimicrobial activity of nanoparticles: present situation and prospects for the future. *International Journal of Nanomedicine*. **2017**, *12*, 1227-1249, https://doi.org/10.2147/IJN.S121956.
37. Roe, A.J.; Byrne, C.O.; McLaggan, D.; Booth, I.R. Inhibition of Escherichia coli growth by acetic acid: a problem with methionine biosynthesis and homocysteine toxicity. *Microbiology*. **2002**, *148*, 2215-2222, https://doi.org/10.1099/00221287-148-7-2215.
38. Gill, E.E.; Franco, O. L.; Hancock, R. Antibiotic adjuvants: diverse strategies for controlling drug-resistant pathogens. *Chemical Biology and Drug Design*. **2015**, *85*, 56-78, https://doi.org/10.1111/cbdd.12478.
39. Savijoki, K.; Skogman, M.; Fallarero, A.; Nyman, T. A.; Sukura, A.; Vuorela, p.; Varmanen, P. Penicillin G increases the synthesis of a suicidal marker (CidC) and virulence (HIgBC) protein in staphylococcus aureus biofilm cells. *International Journal of Medical Microbiology*. **2016**, *306*, 69-74, https://doi.org/10.1016/j.ijmm.2015.11.006.
40. Liarrull, L.I.; Fisher, J.F.; Mobashery, S. Molecular basis and phenotype of methicillin resistant in *staphylococcus aureus* and insight into new β-lactams that meet challenge. *American Society for Microbiology*. **2009**, *53*, 4051-4063, https://doi.org/10.1128/AAC.00084-09.
41. Nagakubo, T.; Tahara, Y.O.; Miyata, M.; Nomura, N.; Toyofuku, M. Mycolic acid-containing bacteria trigger distinct types of membrane vesicles through different routes. *iScience*. **2021**, *24*, 1-57, https://doi.org/10.1016/j.isci.2020.102015.
42. Zeng, X.; Lin, J. Beta-lactamase induction and cell wall metabolism in Gram-negative bacteria. *Frontiers in Microbiology*. **2013**, *4*, 1-9, https://doi.org/10.3389/fmicb.2013.00128.
43. Fergestad, M.E.; Stamsås, G.A.; Morales, A,D.; Salehian, Z.; Wasteson, Y.; Kjos, M. Penicillin-binding protein PBP2a provides variable levels of protection toward different β-lactams in *Staphylococcus aureus* RN4220. *MicrobiologyOpen*. **2020**, *1*, 1-11, https://doi.org/10.1002/mbo3.1057.
44. Kim, J.J.A.; Chukeatirote, E.; Ahn, J. Assessment of antibiotic resistance klebsiella pneumonia exposed to sequential in vitro antibiotic treatments. *Annals of Clinical Microbiology and Antimicrobials*. **2016**, *15*, 1-7, https://doi.org/10.1186/s12941-016-0173-x.
45. Lade, H.; Kim, J.S. Bacterial targets of antibiotics in Methicillin-Resistant *Staphylococcus aureus*. *Antibiotics*. **2021**, *10*, 398-426, https://doi.org/10.3390/antibiotics10040398.
46. Panchal, V.V.; Griffiths, C.; Mosaei, H.; Bilyk, B.; Sutton, J.A.F.; Carnell, O.T.; Hornby, D.P.; Green, J.; Hobbs, J.K.; Kelley, W.L.; Zenkin, N.; Foster, S.J.; Peschel, A. Evolving MRSA: High-level β-lactam resistance in *Staphylococcus aureus* is associated with RNA Polymerase alterations and fine tuning of gene expression. *PLOS Pathogens*. **2020**, *16*, 1-29, https://doi.org/10.1371/journal.ppat.1008672.
47. Wei, Z.; Xiao, C.; Guo, C.; Zhang, X.; Wang, Y.; Wang, J.; Yang, Z.; Fu, Y. Sodium acetate inhibits Staphylococcus aureus internalization into bovine mammary epithelial cells by inhibiting NF-κB activation. *Microbial Pathogenesis*. **2017**, *107*, 116–121, https://doi.org/10.1016/j.micpath.2017.03.030.